

Uptake of Organic Gas Phase Species by 1-Methylnaphthalene

H. Z. Zhang[†] and P. Davidovits*

Chemistry Department, Boston College, Chestnut Hill, Massachusetts 02467

L. R. Williams, C. E. Kolb, and D. R. Worsnop

Center for Chemical and Environmental Physics, Aerodyne Research Inc., 45 Manning Road, Billerica, Massachusetts 01821

Received: January 18, 2005; In Final Form: March 4, 2005

Organic compounds are a significant component of tropospheric aerosols. In the present study, 1-methylnaphthalene was selected as a surrogate for aromatic hydrocarbons (PAHs) found in tropospheric aerosols. Mass accommodation coefficients (α) on 1-methylnaphthalene were determined as a function of temperature (267 K to 298 K) for gas-phase *m*-xylene, ethylbenzene, butylbenzene, α -pinene, γ -terpinene, *p*-cymene, and 2-methyl-2-hexanol. The gas uptake studies were performed with droplets maintained under liquid–vapor equilibrium conditions using a droplet train flow reactor. The mass accommodation coefficients for all of the molecules studied in these experiments exhibit negative temperature dependence. The upper and lower values of α at 267 and 298 K respectively are as follows: for *m*-xylene 0.44 ± 0.05 and 0.26 ± 0.03 ; for ethylbenzene 0.37 ± 0.03 and 0.22 ± 0.04 ; for butylbenzene 0.47 ± 0.06 and 0.31 ± 0.04 ; for α -pinene 0.47 ± 0.07 and 0.10 ± 0.05 ; for γ -terpinene 0.37 ± 0.04 and 0.12 ± 0.06 ; for *p*-cymene 0.74 ± 0.05 and 0.36 ± 0.07 ; for 2-methyl-2-hexanol 0.44 ± 0.06 and 0.29 ± 0.06 . The uptake measurements also yielded values for the product $HD_1^{1/2}$ for most of the molecules studied (H = Henry's law constant, D_1 = liquid-phase diffusion coefficient). Using calculated values of D_1 , the Henry's law constants (H) for these molecules were obtained as a function of temperature. The H values at 298 K in units 10^3 M atm^{-1} are as follows: for *m*-xylene (0.48 ± 0.05); for ethylbenzene (0.50 ± 0.08); for butylbenzene (3.99 ± 0.93); for α -pinene (0.53 ± 0.07); for *p*-cymene (0.23 ± 0.07); for 2-methyl-2-hexanol (1.85 ± 0.29).

Introduction

Organic compounds are abundant in many regions of the troposphere and represent a significant mass fraction of tropospheric particles. For example, fine particle (diameter less than $2 \mu\text{m}$) composition studies showed that, in the United States, organic compounds represent approximately 30% of fine particulate mass in the eastern United States (both in urban and rural locations) and between 30% and 80% mass in urban areas of the western United States.¹ Based on the available measurements, Liou et al.² reported that the calculated average organic submicrometer particle concentration is $0.5\text{--}2 \mu\text{g m}^{-3}$ in the United States. This figure is as high as $10\text{--}12 \mu\text{g m}^{-3}$ in central Europe, the Amazon basin, west central Africa, eastern China, and northern Australia.²

It is now recognized that organic compounds play an important role in chemical balance, cloud formation, radiative forcing, and health effects in the atmosphere.^{1,3–5} For example, Zimmerman and co-workers⁶ estimated that approximately 480 Tg of terpenes are emitted as gases each year from natural sources. The terpenes are a significant sink for ozone during nighttime hours and during periods of high organic emission.¹ Organic matter can significantly contribute to the mass of cloud condensation nuclei (CCN) particles³ and thus also indirectly affect the atmospheric radiative budget. During the past decade, considerable phenomenological information has been gathered

about inorganic aerosols. However, much about the formation, evolution, and important interactions of organic aerosol particles remains unknown.^{1,7}

Organic compounds in atmospheric aerosols cover a wide range of species with widely varying solubilities, reactivities, and physical properties. This complexity makes them difficult to identify.^{1,8,9} In the face of such complexity, to obtain basic information about the atmospheric behavior of organics, in laboratory experiments one must study surrogate compounds representing classes of organic species found in aerosols.¹⁰

In our previous studies of gas uptake by organic liquids, we chose ethylene glycol as a surrogate for hydrophilic organic compounds¹¹ and 1-octanol as surrogate for hydrophobic oxygenated organic compounds.^{12,13} We measured uptake of gas-phase HCl and HBr on pure ethylene glycol and on ethylene glycol–water solutions as a function of water mole fraction (0–1) under liquid–vapor equilibrium conditions. On the 1-octanol surface, we measured the uptake of several atmospherically relevant organic gases, gas-phase hydrogen halides (HCl, HBr, HI) and acetic acid. The uptake was measured as a function of temperature and relative humidity. The uptake studies yielded the mass accommodation coefficient (α) for the species, defined as the probability that a gaseous molecule striking a liquid surface enters into the bulk liquid phase. This parameter is of fundamental importance to the understanding of interactions of gas molecules with a liquid surface. The experiments also yielded Henry's law solubility constants and provided informa-

* To whom correspondence should be addressed.

[†] Current address: Mykrolis Corporation, 129 Concord Road, Billerica, MA 01821.

tion about the nature of both hydrophilic and hydrophobic organic surfaces as a function of relative humidity.

In the present study, 1-methylnaphthalene was selected as a surrogate for polycyclic aromatic hydrocarbons (PAHs) found in tropospheric aerosol particles. Polycyclic aromatic hydrocarbons are produced by high-temperature reactions, such as incomplete combustion of fossil fuels. PAH compounds are one of the major toxic organic constituents found in aerosols.¹⁴ The PAHs undergo thermal decomposition and react with a number of atmospheric chemicals resulting in products which can be more toxic than the original compounds.¹⁵

1-Methylnaphthalene is a hydrophobic, low vapor pressure liquid. Its vapor pressure at 298 K is 0.068 Torr. The solubility of 1-methylnaphthalene in water is 25.8 mg L⁻¹ at 298 K.¹⁶ However, 1-methylnaphthalene is soluble in benzene, ether, and alcohol.¹⁷

Using a droplet train apparatus, uptake on 1-methylnaphthalene was studied as a function of temperature (267–298 K) for the organic gas-phase species *m*-xylene, ethylbenzene, butylbenzene, α -pinene, γ -terpinene, *p*-cymene, and 2-methyl-2-hexanol. The experiments yielded the mass accommodation coefficients for each species as a function of temperature (267–298 K). The uptake measurements also yielded values for the product $HD_1^{1/2}$ for most of the molecules studied (H = Henry's law constant, D_1 = liquid-phase diffusion coefficient). Using calculated values of D_1 , the Henry's law constants (H) for these molecules were obtained.

The aromatic hydrocarbons *m*-xylene, ethylbenzene, and butylbenzene are emitted by combustion of a variety of hydrocarbon fuels^{18–20} and wood burning.²¹ The average gas-phase concentration of xylene (*m*-xylene + *p*-xylene) and ethylbenzene was measured to be 4.3 ppb in southern California,²² which was 21% in mass of the total gas-phase aromatic compounds measured in the same study.

The monoterpenes are emitted into the atmosphere by various evergreen trees. The atmospheric concentration of monoterpenes was observed to be as high as 2.9 ppbv in a fir forest.²³ The molecule 2-methyl-2-hexanol was selected as a convenient surrogate for biogenic alcohols, such as 2-methyl-3-buten-2-ol (MBO),²⁴ (3*Z*)-hexenol,²⁵ and *n*-hexanol,²⁶ which are also emitted by evergreens and certain types of oak.

Gas–Liquid Interactions

In the absence of surface reactions, the mass accommodation coefficient limits the maximum flux, J , of gas into a liquid, which is given by

$$J = \frac{n_g \bar{c} \alpha}{4} \quad (1)$$

Here n_g is the molecular density of the gas molecules of interest and \bar{c} is their average thermal speed. If reactions occur at the gas–liquid interface, then the flux of species disappearing from the gas phase may exceed that given by eq 1. Of course, the flux cannot exceed the collision rate ($n_g \bar{c}$)/4.

Two additional effects limit the net flux. First, as the gas molecules enter the liquid, new molecules have to move toward the liquid surface to replenish the depleted region near the liquid surface. The rate of transport toward the liquid surface is determined by gas-phase diffusion that can limit the rate of uptake by the liquid. Second, as the gas-phase species enters the bulk liquid, a fraction evaporates back into the gas phase. This process is governed by gas/liquid partitioning. In experiments subject to these effects, the measured flux (J_{meas}) into a

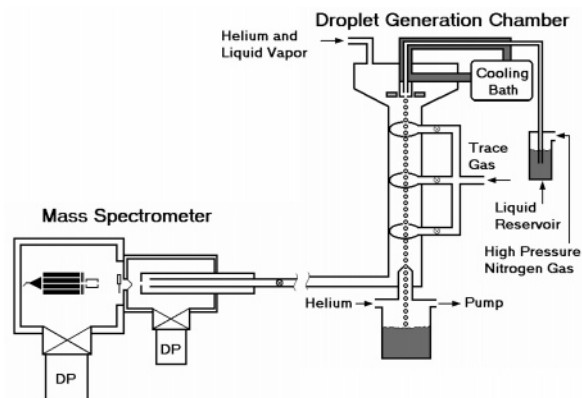


Figure 1. Schematic of the droplet train flow reactor apparatus. (Reprinted with permission from Nathanson et al., 1996. Copyright 1996, American Chemical Society.)

surface may be expressed in terms of a measured uptake coefficient, γ_{meas}

$$J_{\text{meas}} = \frac{n_g \bar{c} \gamma_{\text{meas}}}{4} \quad (2)$$

To a good approximation these effects can be de-coupled, and γ_{meas} can be expressed as

$$\frac{1}{\gamma_{\text{meas}}} = \frac{1}{\Gamma_{\text{diff}}} + \frac{1}{\alpha} + \frac{1}{\Gamma_{\text{sat}}} \quad (3)$$

Γ_{sat} takes into account evaporation of trace gas molecules that have entered the bulk liquid phase (i.e., Γ_{sat} represents the effect of gas/liquid partitioning). Γ_{sat} can be approximated by the expression used and validated in our previous studies:^{12,27}

$$\frac{1}{\Gamma_{\text{sat}}} = \frac{\bar{c}}{8RTH} \sqrt{\frac{\pi t}{D_1}} \quad (4)$$

Here D_1 is the liquid-phase diffusion coefficient of the species in 1-methylnaphthalene, t is the gas–liquid interaction time, R is the gas constant in unit L atm K⁻¹ mol⁻¹, T is temperature, and H (M atm⁻¹) is the Henry's law constant. Note that Γ_{sat} measures the extent to which the gas-phase species is out of equilibrium with the liquid. As equilibrium is approached, Γ_{sat} approaches 0.

The parameter Γ_{diff} takes into account the effect of gas-phase diffusion on the uptake. It has been demonstrated that a modified Fuchs–Sutugin formulation^{28–30} for Γ_{diff} takes into account appropriately the effect of gas-phase diffusion on the uptake as

$$\frac{1}{\Gamma_{\text{diff}}} = \frac{0.75 + 0.283Kn}{Kn(1 + Kn)} \quad (5)$$

Here, Kn is the Knudsen number defined as $2\lambda/d_f$, where λ is the gas-phase mean free path and d_f represents the diameter of the droplets. The mean free path is here expressed as $\lambda = 3D_g/\bar{c}$, where D_g is the gas-phase diffusion coefficient of the species. For the droplet train apparatus, $d_f = (2.0 \pm 0.1)d_o$, where d_o is the diameter of the droplet-forming orifice.³⁰

Experimental Description

In the droplet train apparatus shown in Figure 1,^{27,31} a fast-moving monodisperse, spatially collimated train of droplets is produced by forcing a liquid through a vibrating orifice located in a separate chamber. In this experiment, the liquid is 1-methylnaphthalene obtained from Sigma-Aldrich Inc. A GC–

mass spectrometric measurement has shown its purity to be better than 99%. The speed of the liquid droplets is in the range of 1500–2800 cm s⁻¹ determined by the orifice diameter and the pressure of the gas that forces the liquid through the orifice. The droplet train passes through a ~30 cm long, 1.4 cm diameter, longitudinal low pressure (2–19 Torr) flow reactor that contains the trace gas species, in this case α -pinene, γ -terpinene, *p*-cymene, 2-methyl-2-hexanol, *m*-xylene, ethylbenzene, or butylbenzene at a density between 2×10^{13} and 3×10^{14} cm⁻³. The flow tube wall is heated to about 50 °C to improve the stability of the experiment.

The trace gas is entrained in a flowing mixture of an inert gas (usually helium) and 1-methylnaphthalene vapor at equilibrium pressure with the liquid 1-methylnaphthalene droplets. The trace gas is introduced through one of three loop injectors located along the flow tube. By selecting the gas inlet port and the droplet velocity, the gas-droplet interaction time can be varied between about 2 and 15 ms.

Depending on the frequency of orifice vibration and the liquid flow rate, the 70 μ m diameter orifice used in this study generates droplets with diameters in the range of 150–300 μ m. Droplet formation frequencies range from 6 to 56 kHz. The uniformity of the droplets, and the droplet velocity along the flow tube are monitored by passing cylindrically focused He–Ne laser beams through the droplet train at three heights along the flow tube.³¹ The droplet velocity along the flow tube is measured to be constant to within 3%. Note that these droplets are large enough that their curvature has a negligible effect on the equilibrium vapor pressure.

The diameter, and hence the surface area of the droplets passing through the flow tube is changed in a stepwise fashion by changing the driving frequency applied to the piezo ceramic in contact with the droplet forming orifice. The density of the trace gas is monitored with a quadrupole mass spectrometer. The uptake coefficient (γ_{meas}) as defined by eq 2 is calculated from the measured change in trace gas signal via eq 6.³¹

$$\gamma_{\text{meas}} = \frac{4F_g}{\bar{c} \Delta A} \ln \frac{n_g}{n'_g} \quad (6)$$

Here F_g is the carrier-gas volume flow rate (~100–500 cm³ s⁻¹) through the system, $\Delta A = A_1 - A_2$ is the change in the total droplet surface area in contact with the trace gas, and n_g and n'_g are the trace gas densities at the outlet of the flow tube after exposure to droplets of area A_2 and A_1 , respectively.

An important aspect of the experimental technique is the careful control of all of the conditions within the apparatus, especially the 1-methylnaphthalene vapor pressure in the droplet generation chamber and in the flow tube. Experiments with 1-methylnaphthalene were performed between 267 and 298 K where the equilibrium 1-methylnaphthalene vapor pressure varies from 0.004 to 0.068 Torr. The liquid 1-methylnaphthalene delivery lines were cooled to the desired droplet temperature. The temperature of the droplets in the reaction zone is maintained by introducing a partial pressure of 1-methylnaphthalene equal to the equilibrium vapor pressure at the droplet temperature.³¹ The required equilibrium 1-methylnaphthalene vapor is produced by bubbling helium gas through the liquid 1-methylnaphthalene in a temperature controlled bubbler and flowing the gas into the droplet generation region at the entrance of the flow tube reactor.

To minimize the effect of gas phase diffusion, uptake is usually measured at the lowest possible overall gas pressure. Because the equilibrium vapor pressure of 1-methylnaphthalene

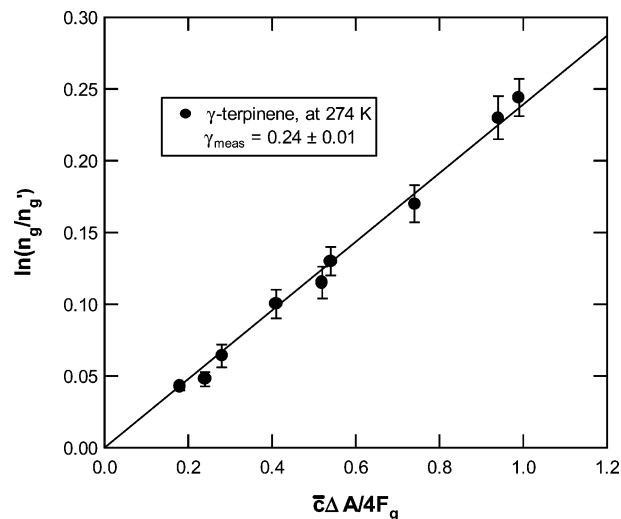


Figure 2. Plot of $\ln(n_g/n'_g)$ as a function of $\bar{c} \Delta A / 4 F_g$, for γ -terpinene at droplet temperature $T_d = 274$ K. Solid line is the least-squares fit to the data. The slope of the line is γ_{meas} . Terms are defined in the text.

is low (only about 0.068 Torr at 298 K), the lowest operating pressure in the flow tube is set by the necessary inert carrier gas flow, which is about 6 Torr of helium.

As shown in Figure 1, the gas-phase molecules are monitored by a mass spectrometer. In all cases, the uptake of the gas-phase species is monitored by a mass spectral line that does not overlap with the mass spectrum of methylnaphthalene.

Overall pressure balance in the flow tube was checked by monitoring simultaneously both the trace species studied and the concentration of an inert reference trace gas, in this case Xe. This gas is effectively insoluble in the liquid droplets. Any change in the reference gas concentration with droplet switching determines the “zero” of the system and was subtracted from observed changes in trace gas concentration. In the present experiments, this correction was always less than 5%.

Results and Analysis

Uptake Coefficients (γ_{meas}). As an example of experimental data, we show in Figure 2 a plot of $\ln(n_g/n'_g)$ for γ -terpinene (274 K) as a function of $\bar{c} \Delta A / 4 F_g$. Here $\bar{c} \Delta A / 4 F_g$ was varied by changing the gas flow rate and the droplet surface area (ΔA). Each point in the figure is the average of at least 10 area change cycles. In all figures, the error bars represent one standard deviation from the mean in the experimentally determined values. As is evident from eq 6, the slope of the line in Figure 2 yields the value of γ_{meas} , in this case with a precision of ~5%. These data yield: $\gamma_{\text{meas}} = 0.24 \pm 0.01$ for γ -terpinene. Similar plots were obtained for a wide range of experimental parameters, for which the uptake fraction, $(n_g - n'_g)/n_g$ varied from 3% to 50%. As is evident in eq 2, γ_{meas} includes the effect of solubility and gas-phase diffusion via Γ_{sat} and Γ_{diff} .

We tested the effect of water vapor on the uptake of gas-phase *p*-cymene at 275 K. The uptake coefficient was measured with the trace gas in a pure helium carrier flow at 7.6 Torr and with 3.4 Torr of water vapor added to the flow. Our usual treatment of gas-phase resistance via eq 5 recovered the same uptake coefficient $\gamma_o = 0.35 \pm 0.02$ to better than 5%.

Uptake of the gas-phase species H₂O, O₃, and HCl was also studied and was found to be below the detection limit of the droplet apparatus. This implies that the uptake coefficient, γ_{meas} , for these species is less than 10^{-3} for trace gas/liquid droplet interaction times up to 1.5×10^{-2} seconds.

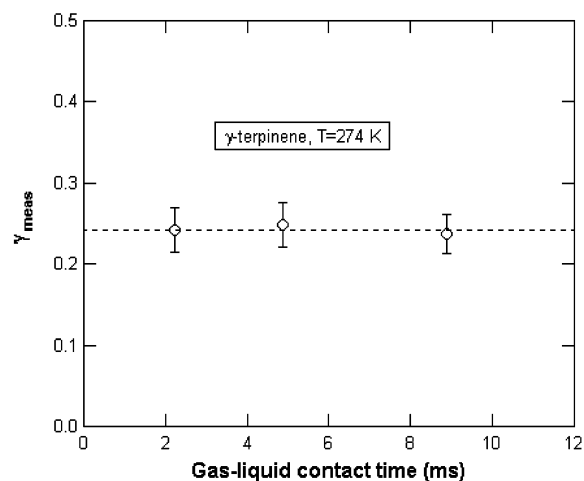


Figure 3. Uptake coefficient γ_{meas} for γ -terpinene as a function of gas–liquid contact time at droplet temperature $T_d = 274$ K. Dashed line is the best straight-line fit to the data.

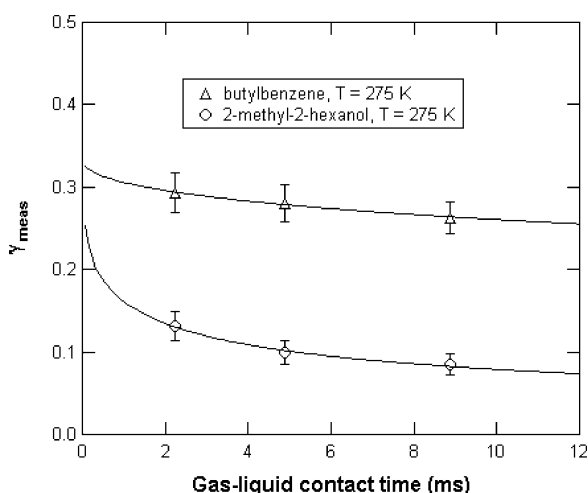


Figure 4. Uptake coefficient γ_{meas} for butylbenzene and 2-methyl-2-hexanol as a function of gas–liquid contact time at droplet temperature $T_d = 275$ K. Solid lines are the best fit to the data via eqs 3 and 4.

Solubility. In Figure 3, γ_{meas} for γ -terpinene on 1-methylnaphthalene at 274 K is plotted as a function of gas–droplet contact time. As is evident, on the scale of the experimental gas–liquid interaction time, the uptake of gas phase γ -terpinene is time-independent. That is, referring to eq 3, $1/\Gamma_{\text{sat}}$ is negligible compared to $(1/\Gamma_{\text{diff}} + 1/\alpha)$. Similar plots were obtained at all other temperatures studied.

In contrast to γ -terpinene, the uptake coefficients γ_{meas} for the other gas-phase species in this study are time dependent indicating that the solubility term $1/\Gamma_{\text{sat}}$ in eq 3 is significant. As an example of time dependent uptake in Figure 4, we show γ_{meas} as a function of gas–droplet contact time for butylbenzene and 2-methyl-2-hexanol at 275 K.

For the species studied in this work, values for the coefficients H and D_1 are not available in the literature. The product $HD_1^{1/2}$ is obtained by optimal fitting of the experimentally determined time dependent γ_{meas} data via eqs 3 and 4. The solid lines in Figure 4 are such plots of γ_{meas} yielding values for $HD_1^{1/2}$. The best fit to the data in Figure 4 yields $HD_1^{1/2} = 26.6 \pm 1.50$ M cm/(atm s^{1/2}) for butylbenzene and 2.32 ± 0.24 M cm/(atm s^{1/2}) for 2-methyl-2-hexanol. Similar plots were obtained at the other temperatures and for all the molecules studied. The fitting procedure also yields γ_{meas} at $t = 0$ which is $(1/\alpha + 1/\Gamma_{\text{diff}})$.

TABLE 1: Measured Values of $HD_1^{1/2}$ for *m*-Xylene, Ethylbenzene, Butylbenzene, α -Pinene, *p*-Cymene, and 2-Methyl-2-hexanol on 1-Methylnaphthalene Droplets at the Temperatures Shown^a

gases	$HD_1^{1/2}$ (M cm atm ⁻¹ s ^{-1/2})			
	265 K	267 K	275 K	298 K
<i>m</i> -xylene	4.26 ± 0.22		3.07 ± 0.12	1.05 ± 0.02
ethylbenzene	3.46 ± 0.16	3.57 ± 0.28	2.79 ± 0.14	1.08 ± 0.08
butylbenzene		41.9 ± 0.50	26.6 ± 1.50	8.00 ± 1.10
2-methyl-2-hexanol		3.14 ± 0.22	2.32 ± 0.24	1.10 ± 0.05
α -pinene		4.12 ± 0.64	2.45 ± 0.20	0.47 ± 0.09
<i>p</i> -cymene		10.2 ± 0.59	10.9 ± 0.88	3.70 ± 0.25

^a Quoted errors are one standard deviation from the mean.

TABLE 2: Values for $(1/\alpha + 1/\Gamma_{\text{diff}})$ for *m*-Xylene, Ethylbenzene, Butylbenzene, α -Pinene, *p*-Cymene, and 2-Methyl-2-hexanol in 1-Methylnaphthalene at the Temperatures Shown^a

gases	$1/\alpha + 1/\Gamma_{\text{diff}}$			
	265 K	267 K	275 K	298 K
<i>m</i> -xylene	2.70 ± 0.16		3.50 ± 0.18	5.05 ± 0.24
ethylbenzene	3.12 ± 0.17	3.15 ± 0.26	4.18 ± 0.23	5.71 ± 0.71
butylbenzene		2.72 ± 0.20	3.01 ± 0.03	4.43 ± 0.28
2-methyl-2-hexanol		2.86 ± 0.27	3.22 ± 0.49	4.53 ± 0.02
α -pinene		2.57 ± 0.42	4.24 ± 0.44	11.9 ± 3.50
<i>p</i> -cymene		1.98 ± 0.08	1.99 ± 0.09	3.98 ± 0.23

^a Quoted errors are one standard deviation from the mean.

TABLE 3: Calculated Values of Liquid Phase Diffusion Coefficients (D_1) for *m*-Xylene, Ethylbenzene, Butylbenzene, α -Pinene, *p*-Cymene, and 2-Methyl-2-hexanol in 1-Methylnaphthalene at the Temperatures Shown^a

gases	D_1 (10^{-6} cm ² s ⁻¹)			
	265 K	267 K	275 K	298 K
<i>m</i> -xylene	1.60		2.39	4.69
ethylbenzene	1.63	1.75	2.40	4.70
butylbenzene		1.62	2.05	4.01
2-methyl-2-hexanol		1.73	2.21	4.23
α -pinene		1.60	2.13	4.24
<i>p</i> -cymene		1.62	2.39	4.01

^a Note: The accuracy of D_1 is $\pm 15\%$.

The uptake coefficients γ_{meas} for *m*-xylene, ethylbenzene, α -pinene, and *p*-cymene are likewise time-dependent on the scale of the experimental gas–liquid interaction time. The products $HD_1^{1/2}$ and the values for $(1/\alpha + 1/\Gamma_{\text{diff}})$ obtained for the species via fitting of the time dependent γ_{meas} are shown in Tables 1 and 2 respectively.

Although the liquid-phase diffusion coefficients D_1 for the gas-phase species studied in this work have not been measured, values for this parameter can be calculated from the Hayduk–Minhas correlation³² with an estimated accuracy of about 15%. Details of the calculations for these species are given in Appendix 2 of Zhang et al.¹² The values of D_1 obtained in this way are listed in Table 3. Using these values for D_1 , the Henry's law coefficients H were computed from the measured values of $HD_1^{1/2}$. The resulting values of H are listed in Table 4. The uncertainties in the H values were estimated by taking account of the uncertainties in D_1 and $HD_1^{1/2}$.

The Henry's law constant (H) tabulated in Table 4 can be expressed as a function of temperature

$$\ln H (\text{M/atm}) = A + (B \times 10^3)/T \quad (7)$$

Here T is temperature (K). The constant A and B are tabulated in Table 5. The data in Table 4 are also shown graphically in Figure 5, parts a and b.

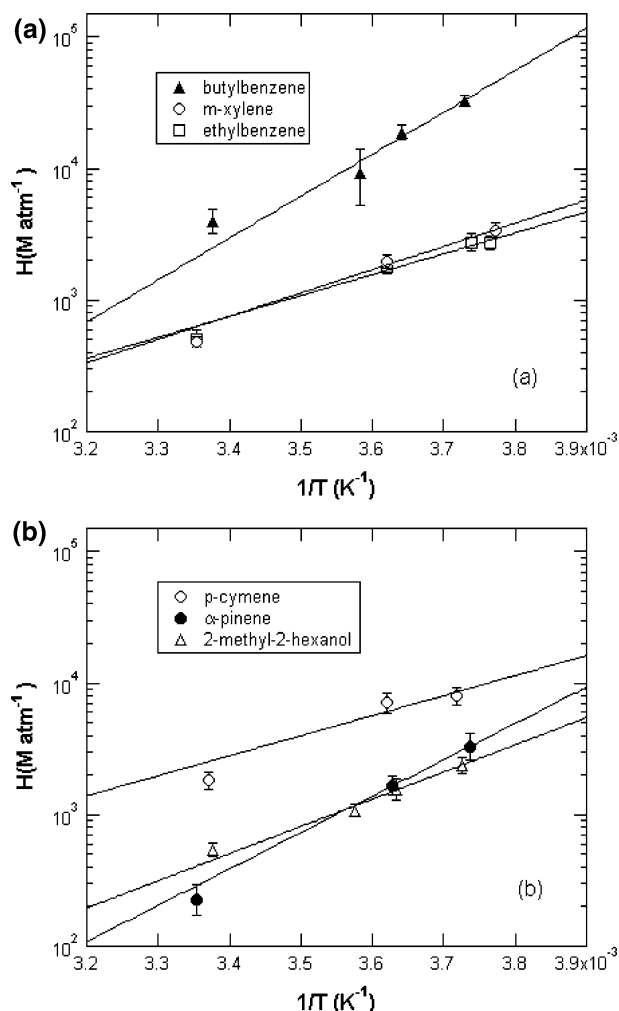


Figure 5. Henry's law solubility (H): (a) for butylbenzene, m -xylene and ethylbenzene; (b) for p -cymene, α -pinene, and 2-methyl-2-hexanol on 1-methylnaphthalene as a function of temperature. Solid lines are obtained via eq 7. H values are also listed in Table 4.

TABLE 4: Henry's Law Constant (H) for m -Xylene, Ethylbenzene, Butylbenzene, α -Pinene, p -Cymene, and 2-Methyl-2-hexanol on 1-Methylnaphthalene at the Temperatures Shown^a

gases	H (10^3 M atm ⁻¹)			
	265 K	267 K	275 K	298 K
m -xylene	3.37 ± 0.47		1.98 ± 0.25	0.48 ± 0.05
ethylbenzene	2.70 ± 0.36	2.69 ± 0.46	1.80 ± 0.25	0.50 ± 0.08
butylbenzene		32.9 ± 3.21	18.6 ± 2.71	3.99 ± 0.93
2-methyl-2-hexanol		2.38 ± 0.38	1.56 ± 0.31	0.53 ± 0.07
α -pinene		3.26 ± 0.83	1.68 ± 0.29	0.23 ± 0.07
p -cymene		8.00 ± 1.18	7.10 ± 1.22	1.85 ± 0.29

^a Quoted errors are one standard deviation from the mean.

TABLE 5: Values of A and B in Equation 7 for m -Xylene, Ethylbenzene, Butylbenzene, α -Pinene, p -Cymene, and 2-Methyl-2-hexanol on 1-Methylnaphthalene

gases	A	B
m -xylene	$-(7.20 \pm 2.17)$	4.06 ± 0.58
ethylbenzene	$-(5.81 \pm 2.08)$	3.66 ± 0.56
butylbenzene	$-(16.9 \pm 3.52)$	7.33 ± 0.95
2-methyl-2-hexanol	$-(9.95 \pm 1.49)$	4.76 ± 0.41
α -pinene	$-(15.7 \pm 1.39)$	6.36 ± 0.37
p -cymene	$-(3.96 \pm 2.40)$	3.51 ± 1.47

Mass Accommodation Coefficient (α). To obtain α , the effect of gas-phase diffusion on the uptake is taken into account by Γ_{diff} calculated from eq 5. Here the gas-phase diffusion

TABLE 6: Gas-Phase Diffusion Coefficients, D_g (atm cm² s⁻¹), Calculated at 298 K

trace gas	carrier gas (He)
m -xylene	0.32
ethylbenzene	0.32
butylbenzene	0.28
2-methyl-2-hexanol	0.31
α -pinene	0.21
γ -terpinene	0.21
p -cymene	0.28

TABLE 7: Mass Accommodation Coefficients (α) for m -Xylene, Ethylbenzene, Butylbenzene, α -Pinene, γ -Terpinene, p -Cymene, and 2-Methyl-2-hexanol at the Temperatures Shown^a

gases	α			
	265 K	267 K	275 K	298 K
m -xylene	0.44 ± 0.05		0.33 ± 0.04	0.26 ± 0.03
ethylbenzene	0.37 ± 0.03	0.37 ± 0.04	0.27 ± 0.05	0.22 ± 0.04
butylbenzene		0.47 ± 0.06	0.43 ± 0.03	0.31 ± 0.04
2-methyl-2-hexanol		0.44 ± 0.06	0.38 ± 0.06	0.29 ± 0.06
α -pinene		0.47 ± 0.07	0.27 ± 0.06	0.10 ± 0.05
γ -terpinene		0.37 ± 0.04	0.32 ± 0.04	0.12 ± 0.06
p -cymene		0.74 ± 0.05	0.67 ± 0.05	0.36 ± 0.07

^a Quoted errors are one standard deviation from the mean.

coefficients D_g used to calculate Kn are obtained using the method described by Reid et al.³² The temperature of the gas for the D_g calculation was assumed to be the average between the wall temperature and the droplet surface temperature.³¹ The values of D_g for the species in He at 298 K are listed in Table 6. The accuracy of these numbers is estimated to be about $\pm 10\%$. Because the experiments were done at a relatively low pressure of He, the gas-phase diffusion correction ($1/\Gamma_{\text{diff}}$) is small. In these studies, $1/\alpha$ is in the range of 1.36–8.13, whereas $1/\Gamma_{\text{diff}}$ is from 0.62 to 3.77, a correction of about 30%. The mass accommodation coefficients (α) for the species studied are listed in Table 7 and are plotted as a function of temperature in Figure 6a–c.

Discussion

Mass Accommodation. As is shown in Figure 6a–c, the mass accommodation coefficients for all of the gas-phase species studied here show negative temperature dependence. A negative temperature dependence for α was observed in our previous uptake studies conducted with about 30 hydrophilic gas-phase species on aqueous surfaces,³³ as well as for HCl, HBr, DCl, and H₂O on ethylene glycol surface¹¹ and HCl, HBr, HI, acetic acid, α -pinene, γ -terpinene, p -cymene, and 2-methyl-2-hexanol on 1-octanol surfaces.^{12,13} As discussed in our previous publications, the mass accommodation coefficient can be expressed as³⁴

$$\frac{\alpha}{1 - \alpha} = \frac{k_{\text{sol}}}{k_{\text{des}}} = \frac{\exp(-\Delta G_{\text{sol}}/RT)}{\exp(-\Delta G_{\text{des}}/RT)} = \exp\left(\frac{\Delta G_{\text{obs}}}{RT}\right) \quad (8)$$

The parameter $\Delta G_{\text{obs}} = \Delta H_{\text{obs}} - T\Delta S_{\text{obs}}$ is the Gibbs energy of the transition state between molecules in the gas phase and molecules solvated in the liquid phase. The values for ΔH_{obs} and ΔS_{obs} can be obtained from the experimental results by plotting $\ln(\alpha/(1 - \alpha))$ as a function of $1/T$. The slope of such a plot is $-\Delta H_{\text{obs}}/R$ and the intercept is $\Delta S_{\text{obs}}/R$. The ΔH_{obs} and ΔS_{obs} values for the species studied are listed in Table 8. (N^* listed in the table is defined below.)

The functional form of ΔG_{obs} depends on the theoretical formulation of the uptake process. Therefore, the parameter

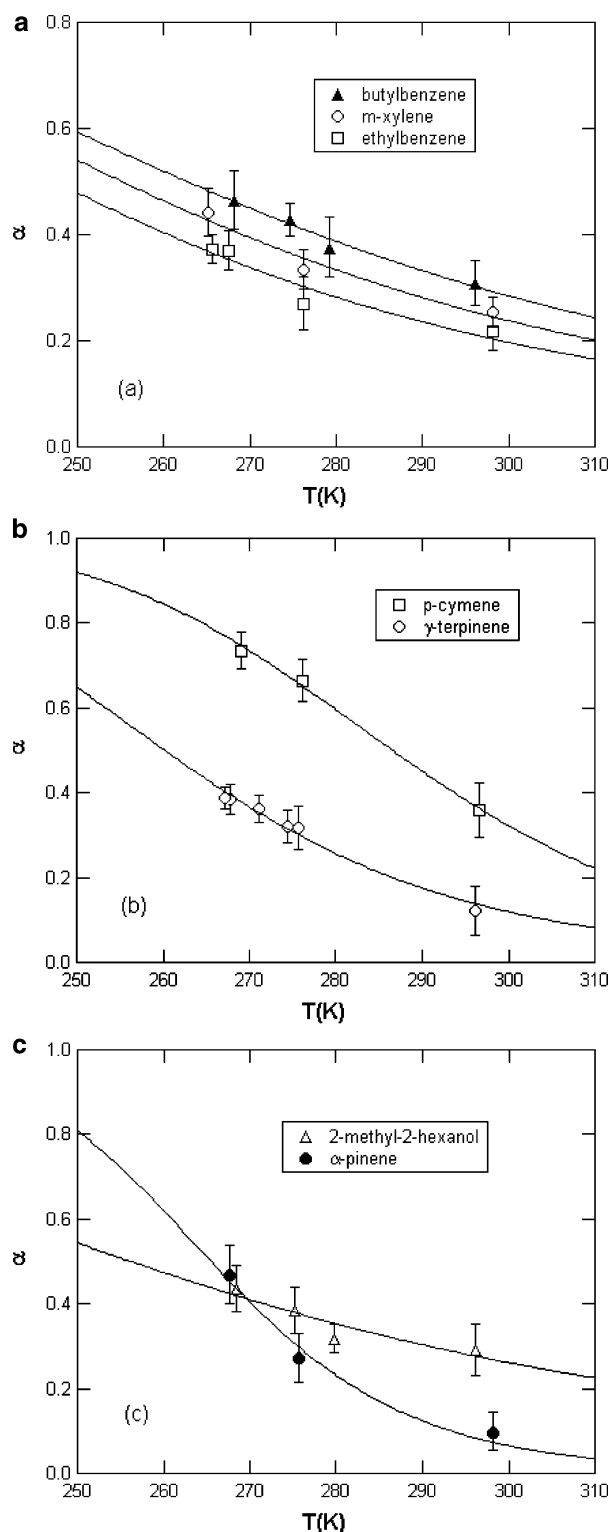


Figure 6. Mass accommodation coefficients (α): (a) for butylbenzene, *m*-xylene and ethylbenzene; (b) for *p*-cymene and γ -terpinene; (c) for α -pinene and 2-methyl-2-hexanol on 1-methylnaphthalene as a function of temperature. Solid lines are obtained via eq 8 with ΔH_{obs} and ΔS_{obs} values listed in Table 8.

ΔG_{obs} serves as a bridge between experiment and theory. Uptake studies on water surfaces led to the formulation of a nucleation-like critical-cluster model for mass accommodation that successfully explained several features noted in our earlier uptake studies on aqueous surfaces including the observation that a plot of ΔH_{obs} versus ΔS_{obs} for all of the species studied exhibits a straight-line relationship.^{34,35} The plot of ΔH_{obs} versus ΔS_{obs}

TABLE 8: ΔH_{obs} , ΔS_{obs} , and N^* for *m*-Xylene, Ethylbenzene, Butylbenzene, α -Pinene, *p*-Cymene, γ -Terpinene, and 2-Methyl-2-hexanol^a

gases	ΔH_{obs} (kcal mol ⁻¹)	ΔS_{obs} cal mol ⁻¹ K ⁻¹)	N^*
<i>m</i> -xylene	$-(3.95 \pm 0.91)$	$-(15.5 \pm 3.3)$	1.65
ethylbenzene	$-(3.93 \pm 0.93)$	$-(15.9 \pm 3.4)$	1.65
butylbenzene	$-(3.87 \pm 0.48)$	$-(14.7 \pm 1.7)$	1.60
2-methyl-2-hexanol	$-(3.62 \pm 1.10)$	$-(14.1 \pm 3.9)$	1.55
α -pinene	$-(12.2 \pm 2.69)$	$-(46.1 \pm 9.9)$	3.38
γ -terpinene	$-(7.79 \pm 0.73)$	$-(29.9 \pm 2.7)$	2.50
<i>p</i> -cymene	$-(9.46 \pm 0.68)$	$-(33.0 \pm 2.4)$	2.75

^a Quoted errors are one standard deviation from the mean.

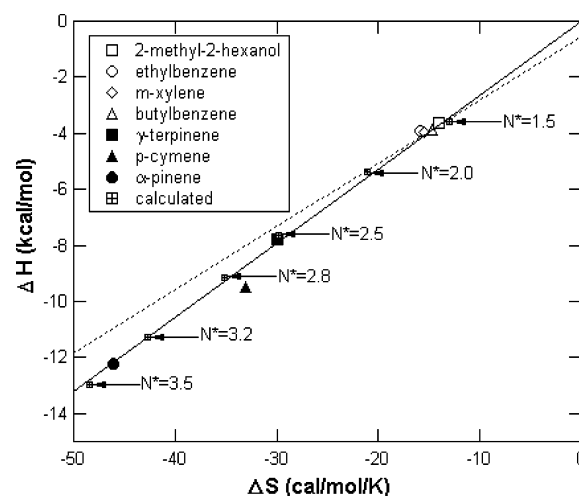


Figure 7. Experimental and calculated values of ΔH_{obs} and ΔS_{obs} for 2-methyl-2-hexanol, ethylbenzene, *m*-xylene, butylbenzene, γ -terpinene, *p*-cymene, α -pinene. Symbols are identified in the figure insert, calculations are shown as crossed squares. The dashed line in the figure is the calculated $\Delta H_{\text{obs}} - \Delta S_{\text{obs}}$ relationship for water.

values for the molecules studied in these 1-methylnaphthalene experiments likewise exhibits a straight-line relationship as is shown in Figure 7. Further, we note that the values of N^* (i.e., ΔH_{obs} and ΔS_{obs}) are not well correlated with the Henry's law constant H . For example, values of N^* for butyl benzene and 2-methyl-2-hexanol are about the same, but H for the alcohol is 0.5 at 298 K, whereas H for butyl benzene is 3.99. This lack of correlation was first noted in our earlier measurements of α for various gas-phase species on water,^{34,35} where we compared ΔH_{obs} and ΔS_{obs} to liquid-phase solubility values ΔH_{sol} and ΔS_{sol} . The observation that the mass accommodation process did not correlate with solubility led to the development of the nucleation model for mass accommodation. The Henry's law constant is determined by the change in enthalpy and entropy for the species between its gas phase and its fully solvated state in the bulk liquid, whereas ΔH_{obs} and ΔS_{obs} , the parameters determining N^* are the enthalpy and entropy changes for the species between its surface adsorbed state and its critical cluster. The observed relationship between ΔH_{obs} and ΔS_{obs} suggests that the critical cluster model of mass accommodation may also apply to uptake on the 1-methylnaphthalene surface.

Brief Description of the Model. In the critical-cluster model, the surface of the liquid is envisioned as a sharp but finite transition region several molecular diameters in thickness within which the density changes from liquid phase to gas phase values. This interface is a dynamic region where small clusters or aggregates of molecules constituting the liquid (in this case 1-methylnaphthalene) are expected to be continually forming, falling apart, and re-forming. The driving force, as described by nucleation theory, is such that clusters smaller than a critical

size (N^*) fall apart, whereas clusters larger than the critical size serve as centers for further aggregation and grow in size until they merge into the adjacent bulk liquid. In this model, gas uptake proceeds via such growth of critical clusters. The incoming gas molecule upon striking the surface becomes a loosely bound surface species that participates in the surface nucleation process. If such a molecule becomes part of a critical sized cluster, it will invariably be incorporated into the bulk liquid via cluster growth.

The ease with which an incoming gas molecule is incorporated into bulk liquid depends on its ability to enter the nucleation or aggregation process with molecules of the liquid at the interface. The critical cluster consists of a specific number of molecules N^* which is the sum of the trace molecule plus the additional number of 1-methylnaphthalene molecules required to form the critical cluster leading to growth and subsequent uptake by the bulk liquid. This number N^* required to form a critical cluster depends on the structure of the specific molecule undergoing the process of uptake. Molecules with the ability to form strong bonds with 1-methylnaphthalene form critical clusters more easily and thus exhibit a smaller N^* .

In the nucleation critical-cluster model of mass accommodation, ΔH_{obs} and ΔS_{obs} can be expressed as^{34,35}

$$\Delta H_{\text{obs}} = (N^* - 1)\Delta H_c + (N^{*2/3} - 1) \left[4\pi E_s N_{\text{Av}} \left(\frac{3V_m}{4\pi N_{\text{Av}}} \right)^{2/3} \right] - \Delta H_{\text{vap.s}} \quad (9)$$

$$\Delta S_{\text{obs}} = (N^* - 1)[\Delta S_c + R \ln(p/MRT)] + (N^{*2/3} - 1) \left[4\pi S_s N_{\text{Av}} \left(\frac{3V_m}{4\pi N_{\text{Av}}} \right)^{2/3} \right] - \Delta S_{\text{vap.s}} \quad (10)$$

Here, N^* is the critical cluster size.

In the expressions for ΔH_{obs} (eq 9) and ΔS_{obs} (eq 10) there are 4 and 5 unknown parameters, respectively. To obtain solutions for ΔH_{obs} and ΔS_{obs} , we must make some reasonable guesses about the values for these parameters. Our choices described below cannot be fully justified nor are they unique, since different combinations yield similar results. The purpose of the calculation is simply to demonstrate that the nucleation model provides a picture of mass accommodation consistent with experimental results.

ΔH_c (eq 9) and ΔS_c (eq 10) are related to the free energy of condensation for the liquid under consideration, in this case 1-methylnaphthalene. That is, $\Delta G_c = \Delta H_c - T\Delta S_c$. ΔG_c is the free energy of transferring a mole of gas phase 1-methylnaphthalene into liquid 1-methylnaphthalene without volume change rather than the usually tabulated standard free energy of condensation. $\Delta G_{\text{vap.s}} = \Delta H_{\text{vap.s}} - T\Delta S_{\text{vap.s}}$ is the free energy of the gas-phase species, n_g , with respect to the surface species, n_s (see ref 33). The parameters E_s and S_s are related to surface tension β expressed as $\beta = E_s - TS_s$. The values of parameters ΔH_c , ΔS_c , E_s , and S_s were calculated by using the data compilation by Daubert and Danner³⁶ and are listed in Table 9.

The pressure parameter p in eq 10 is an equivalent density of 1-methylnaphthalene (i.e., the surface density of methyl naphthalene = p/RT) in the surface region where the incoming trace molecule collides with the interface and is adsorbed. We use the same value for p as was determined from fits to data for aqueous surfaces,³⁵ i.e., $p = 67$ Torr. (This is an arbitrary choice to simplify the calculations.) Then we obtain $R \ln(p/MRT) = -14.9$ for 1-methylnaphthalene. In our calculations we assume that $\Delta G_{\text{vap.s}} = f_1 \Delta H_c - f_2 \Delta S_c T$. (Note that ΔG_{vap}

TABLE 9: Values for Heat (ΔH_c) and Entropy (ΔS_c) of Condensation, and for Surface Energy (E_s) and Entropy (S_s) for 1-Methylnaphthalene^a

1-methylnaphthalene	
ΔH_c (kcal mol ⁻¹)	-14.0
ΔS_c (cal mol ⁻¹ K ⁻¹)	-17.0
E_s (cal cm ⁻²)	1.7×10^{-6}
S_s (cal cm ⁻² K ⁻¹)	2.6×10^{-9}
f_1	0.17
f_2	0.35

^a The parameters f_1 and f_2 related to eqs 9 and 10 are also shown.

TABLE 10: Calculated Values for ΔH_{obs} and ΔS_{obs} Obtained via Equations 11 and 12

N^*	ΔH_{obs} (kcal mol ⁻¹)	ΔS_{obs} (cal mol ⁻¹ K ⁻¹)
1.5	-3.9	-12
2.0	-5.6	-21
2.5	-7.8	-29
2.8	-9.3	-35
3.2	-11	-43
3.5	-13	-48

is the negative of the free energy of condensation, i.e., $\Delta G_{\text{vap}} = -\Delta G_c$.) (See Nathanson 1996³⁵ for a more detailed discussion.)

Equations 9 and 10 now contain two unknown parameters: f_1 and f_2 . Our strategy is to obtain values for f_1 and f_2 for selected values of N^* so as to provide a fit to the set of experimentally determined values of ΔH_{obs} and ΔS_{obs} listed in Table 8. Fitting values of f_1 and f_2 are listed in Table 9. With these and other previously obtained numerical values for the relevant parameters, we obtain

$$\Delta H_{\text{obs}} = -14.0(N^* - 1) + 18.7(N^{*2/3} - 1) - 0.17 \times 14.0 \text{ (kcal M}^{-1}\text{)} \quad (11)$$

$$\Delta S_{\text{obs}} = -17.0(N^* - 1) - 14.9(N^* - 1) + 28.6(N^{*2/3} - 1) - 0.35 \times 17.0 \text{ (cal M}^{-1}\text{ K}^{-1}\text{)} \quad (12)$$

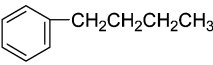
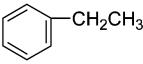
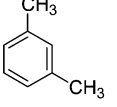
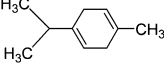
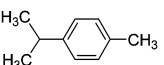
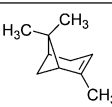
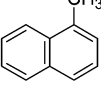
Calculated values of ΔH_{obs} and ΔS_{obs} for selected values of N^* are shown in the Table 10. These values, together with the values obtained from the measurements as listed in Table 8, are plotted in the Figure 7. The solid line is a straight-line fit to the calculated ΔH_{obs} and ΔS_{obs} values shown in the figure as small squared crosses. As is evident, the calculations are in good agreement with the experimental values.

N^* is the number of molecules required to form a critical cluster resulting in entry of the trace gas into the bulk liquid. The smaller the critical cluster size N^* , the greater is the facility of a given trace gas molecule itself to form a critical cluster. Thus, N^* is expected to depend on the structure of the specific molecule undergoing the uptake process. Specifically, we would expect that a trace gas with a structure similar to 1-methylnaphthalene and/or one that exerts a larger attractive force on 1-methylnaphthalene will be associated with the smaller N^* .

These expectations are supported by the data in Table 11 which displays N^* , structure, dipole-moment, and vapor pressure for the organic gases studied. First we note that the N^* values for *m*-xylene, ethylbenzene, butylbenzene, and 2-methyl-2-hexanol are almost the same ($N^* = 1.55$ – 1.65) and small, whereas N^* values for γ -terpinene, *p*-cymene, and α -pinene are larger ranging from 2.50 to 3.38.

The three aromatic compounds with the smaller N^* values all have larger dipole moments and a planar configuration similar to the liquid 1-methylnaphthalene than the molecules in the

TABLE 11: Formula and Structure of Organic Gases Studied and 1-Methylnaphthalene (the Liquid)

Name and Formula	N*	Structure	Dipole Moment (10 ⁻³⁰ C m)	Vapor Pressure (torr, 293K)
2-methyl-2-hexanol C ₇ H ₁₆ O	1.55	CH ₃ (CH ₂) ₃ C(CH ₃) ₂ OH	4.93	1.36
Butylbenzene C ₁₀ H ₁₄	1.60		2.77	0.71
Ethylbenzene C ₈ H ₁₀	1.65		1.97	7.19
m-xylene C ₈ H ₁₀	1.65		1.00	6.30
γ-terpinene C ₁₀ H ₁₆	2.50		<1.00	0.76
p-cymene C ₁₀ H ₁₄	2.75		0.00	1.03
α-pinene C ₁₀ H ₁₆	3.38		1.20	3.54
<u>1-methylnaphthalene</u> C ₁₁ H ₁₀ (the liquid)			1.70	0.05

larger N^* grouping. Furthermore, within the group with smaller N^* , 2-methyl-2-hexanol which has the largest dipole moment, as expected, displays the smallest N^* . Conversely, within this group, *p*-cymene with the smallest dipole moment is associated with a larger N^* .

The molecule α -pinene is associated with the largest N^* in this series. In other words, it is least likely to promote the formation of a critical cluster. This can be understood in terms of the configuration of the molecule. As shown in Table 11, α -pinene has a highly nonplanar configuration that does not match well with planar 1-methylnaphthalene, hindering cluster formation.

Atmospheric Implications. Our results show that the gas-phase organic molecules studied have relatively large mass accommodation coefficients (0.1–0.36 at 298 K) on liquid 1-methylnaphthalene surfaces. This is on the order of Γ_{diff} under atmospheric conditions for a particle about 1 micron in diameter. This implies that for aerosols with significant PAH content, larger than about 1 micron, α is not likely to be a rate determining parameter for the uptake of gas phase organic molecules. The rate-limiting step is likely to be gas-phase diffusion or constraints imposed by Henry's law solubility. However, for aerosols smaller than about 1 micron, the effect of α on the uptake needs to be taken into account.

Acknowledgment. Funding for this work was provided by the National Science Foundation Grants Nos. ATM-0212464 and CH-0089147, by the Biological and Environmental Research Program Department of Energy Grant No. DE-FG02-98ER62581, and by the US-Israel Binational Science Foundation Grant No. 1999134.

References and Notes

- Jacobson, M. C.; Hansson, H.-C.; Noone, K. J.; Charlson, R. J. *Rev. Geophys.* **2000**, *38*, 267.
- Liousse, C.; Penner, J. E.; Chuang, C.; Walton, J. J.; Eddleman, H.; Cachier, H. *J. Geophys. Res. Atmos.* **1996**, *101*, 19411.
- Novakov, T.; Penner, J. E. *Nature* **1993**, *365*, 823.
- Reid, J. P.; Sayer, R. M. *Sci. Prog. Fields* **2002**, *85*, 263.
- Rudich, Y. *Chem. Rev.* **2003**, *103*, 5097.
- Zimmerman, P. R.; Chatfield, R. B.; Fishman, J.; Crutzen, P. J.; Hanst, P. L. *Geophys. Res. Lett.* **1978**, *5*, 679.
- Andreae, M. O.; Crutzen, P. J. *Science* **1997**, *276*, 1052.
- Saxena, P.; Hildemann, L. M. *J. Atmos. Chem.* **1996**, *24*, 57.
- Turpin, B. J.; Saxena, P.; Andrews, E. *Atmos. Environ.* **2000**, *34*, 2983.
- Moise, T.; Rudich, Y. *J. Geophys. Res. Atmos.* **2000**, *105*, 14667.
- Li, Y. Q.; Zhang, H. Z.; Davidovits, P.; Jayne, J. T.; Kolb, C. E.; Worsnop, D. R. *J. Phys. Chem. A* **2001**, *106*, 1220.
- Zhang, H. Z.; Li, Y. Q.; Xia, J. R.; Davidovits, P.; Williams, L. R.; Jayne, J. T.; Kolb, C. E.; Worsnop, D. R. *J. Phys. Chem. A* **2003**, *107*, 6388.
- Zhang, H. Z.; Li, Y. Q.; Davidovits, P.; Williams, L. R.; Jayne, J. T.; Kolb, C. E.; Worsnop, D. R. *J. Phys. Chem. A* **2003**, *107*, 6398.
- Lyall, R. J.; Hooper, M. A.; Mainwaring, S. J. *Atmos. Environ.* **1988**, *22*, 2549.
- Nikolaou, K.; Masplet, P.; Mouvier, G. *Sci. Total Environ.* **1984**, *32*, 103.
- Aquasol database of aqueous solubility*; Yaldowsky, S. H.; Dannefeller, R. M., Eds.; University of Arizona: Tucson, AZ, 1992; Vol. Version 5.
- Budavari, S.; O'Neil, M.; Smith, A.; Heckelman, P.; Kinneary, J., Eds.; *The Merck Index*, 12th ed.; Merck and Co.: Whitehouse Station, NJ, 1996.
- Kado, N. Y.; Okamoto, R. A.; Kuzmicky, P. A.; Rathbun, C. J.; Hsieh, D. P. H. *Chemosphere* **1996**, *33*, 495.
- Baker, R. J.; Best, E. W.; Baehr, A. L. *Ground W. Monit. Remed.* **2002**, *22*, 46.

- (20) Seinfeld, J. H.; Pandis, S. N. *Atmospheric Chemistry and Physics: From Air Pollution to Climate Change*; John Wiley & Sons: New York, 1998.
- (21) Rogge, W. F.; Hildemann, L. M.; Mazurek, M. A.; Cass, G. R.; Simoneit, B. R. T. *Environ. Sci. Technol.* **1998**, *32*, 13.
- (22) Fraser, M. P.; Cass, G. R.; Simoneit, B. R. T.; Rasmussen, R. A. *Environ. Sci. Technol.* **1998**, *32*, 1760.
- (23) Harrison, D.; Hunter, M. C.; Lewis, A. C.; Seakins, P. W.; Bonsang, B.; Gros, V.; Kanakidou, M.; Touaty, M.; Kavouras, I.; Mihalopoulos, N.; Stephanou, E.; Alves, C.; Nunes, T.; Pio, C. *Atmos. Environ.* **2001**, *35*, 4699.
- (24) Harley, P.; Fridd-Stroud, V.; Greenberg, J.; Guenther, A.; Vasconcellos, P. *J. Geophys. Res. Atmos.* **1998**, *103*, 25479.
- (25) Arey, J.; Winer, A. M.; Atkinson, R.; Aschmann, S. M.; Long, W. D.; Morrison, C. L. *Atmos. Environ. A* **1991**, *25A*, 1063.
- (26) Fall, R. *Reactive Hydrocarbons in the Atmosphere*; Academic Press: San Diego, CA, 1999.
- (27) Shi, Q.; Davidovits, P.; Jayne, J. T.; Worsnop, D. R.; Kolb, C. E. *J. Phys. Chem. A* **1999**, *103*, 8812.
- (28) Jayne, J. T.; Duan, S. X.; Davidovits, P.; Worsnop, D. R.; Zahniser, M. S.; Kolb, C. E. *J. Phys. Chem.* **1991**, *95*, 6329.
- (29) Shi, Q. Gas-Liquid Interactions of Ammonia, Sulfur Dioxide, Hydrogen Sulfide, Deuterated Acetic Acid and Ethanol on Aqueous Surfaces. Ph.D. Thesis, Boston College: Chestnut Hill, MA, 1998.
- (30) Worsnop, D. R.; Shi, Q.; Jayne, J. T.; Kolb, C. E.; Swartz, E.; Davidovits, P. *J. Aerosol Sci.* **2001**, *32*, 877.
- (31) Worsnop, D. R.; Zahniser, M. S.; Kolb, C. E.; Gardner, J. A.; Watson, L. R.; Van Doren, J. M.; Jayne, J. T.; Davidovits, P. *J. Phys. Chem.* **1989**, *93*, 1159.
- (32) Reid, R. C.; Prausnitz, J. M.; Poling, B. E. *The Properties of Gases and Liquids*; McGraw Hill: New York, 1987.
- (33) Kolb, C. E.; Davidovits, P.; Worsnop, D. R.; Shi, Q.; Jayne, J. T. *Prog. Kinet. Mech.* **2002**, *27*, 1.
- (34) Davidovits, P.; Jayne, J. T.; Duan, S. X.; Worsnop, D. R.; Zahniser, M. S.; Kolb, C. E. *J. Phys. Chem.* **1991**, *95*, 6337.
- (35) Nathanson, G. M.; Davidovits, P.; Worsnop, D. R.; Kolb, C. E. *J. Phys. Chem.* **1996**, *100*, 13007.
- (36) *Physical and thermodynamic properties of pure chemicals: data compilation*; Daubert, T. E., Danner, R. P., Eds.; Hemisphere Publishing Corporation: New York, 1989.